World Neurosurgery: X 19 (2023) 100199

Contents lists available at ScienceDirect

World Neurosurgery: X

journal homepage: www.journals.elsevier.com/world-neurosurgery-x

Finite element analysis of short and long posterior spinal instrumentation and fixation for different pathological thoracolumbar vertebral fractures

Norihiro Nishida [a,*], Fei Jiang [b], Rei Kitazumi [b], Yuto Yamamura [b], Takahiro Asano [b], Rui Tome [b], Yogesh Kumaran [c], Hidenori Suzuki [a], Masahiro Funaba [a], Junji Ohgi [b], Xian Chen [b], Takashi Sakai [a]

[a] Department of Orthopedic Surgery, Yamaguchi University Graduate School of Medicine, 1-1-1 Minami-Kogushi, Ube City, Yamaguchi Prefecture, 755-8505, Japan
[b] Faculty of Engineering, Yamaguchi University, 2-16-1 Tokiwadai, Ube City, Yamaguchi, 755-8611, Japan
[c] Engineering Center for Orthopaedic Research Excellence (E-CORE), Departments of Bioengineering and Orthopaedics, The University of Toledo, Toledo, OH, USA

ARTICLE INFO

Keywords:
Finite element method
Vertebral fracture
Stress
Posterior fusion
Instrumentation

1. Introduction

The outcomes of posterior spine fixation surgery for vertebral fractures have recently been improved by minimally invasive surgery (MIS) and instrumentation development, including pedicle screws and rods.[1–3] Short segment fixation, which is less invasive, achieves better outcomes for vertebral fractures. However, many studies suggest that long fusion is more advantageous for lordosis correction and for preservation of segmental lordosis.[4–8] Nevertheless, the length of fixation remains controversial in terms of adjacent segment disease (ASD) after posterior fixation, instrument failure such as rod and screw fractures loosening, and surgical invasiveness.[9–11] Furthermore, the risk of postoperative complications is lower in young patients with solid vertebrae and early fusion than in patients with fractures mainly caused by osteoporosis and underlying conditions, such as diffuse idiopathic skeletal hyperostosis (DISH).[12] Screw loosening and the collapse of the vertebrae after fixation are more common in osteoporotic vertebral fractures. In DISH, the anterior longitudinal ligament (ALL) is cross-linked and ossified between vertebral bodies, which reduces flexibility and concentrates stress on the fracture site; therefore, selecting the correct fixation length is challenging.[13,14] In clinical settings like much of spine surgery, spine surgeons select the length of fixation, choose between open or percutaneous surgery, and assess the need for bone graft, additional anterior fusion, or the use of hooks and taping based on each case. Although various surgical procedures are available, it would be beneficial to the patient if MIS surgery could address the problem. Therefore, it would be helpful for clinicians to visualize the length of fixation for osteoporosis and DISH, which has clinical problems compared to young patients and affects the vertebrae inserted in the screws and instrumentation. A finite element (FE) analysis comparing the length of fixation in posterior spine fusion amongst pathological models can assist in determining the optimal fixation length. Based on a three-dimensional (3D) FE spine model created from medical images and actual screw data, the following four pathological models: the fracture model, osteoporosis fracture model, DISH fracture model, and DISH-osteoporosis fracture model, were used to analyze and compare the effects of spine flexion-extension in pathological conditions on instrumentation and the length of fixation. The present study is the first to use actual screw data and a long spine length to consider pathology and different fixation lengths.

* Corresponding author. Department of Orthopedic Surgery, Yamaguchi University Graduate School of Medicine, 1-1-1 Minami-Kogushi, Ube City, Yamaguchi Prefecture, 755-8505, Japan.

E-mail addresses: nishida3@yamaguchi-u.ac.jp (N. Nishida), fjiang@yamaguchi-u.ac.jp (F. Jiang), i019vdrky@gmail.com (R. Kitazumi), yuto.choco@gmail.com (Y. Yamamura), takahiroasano112740@gmail.com (T. Asano), rui.t.19940116@gmail.com (R. Tome), yogesh.kumaran@rockets.utoledo.edu (Y. Kumaran), hhhsuzuki7@gmail.com (H. Suzuki), funa51.mf@gmail.com (M. Funaba), ohgi@yamaguchi-u.ac.jp (J. Ohgi), xchen@yamaguchi-u.ac.jp (X. Chen), cozy@yamaguchi-u.ac.jp (T. Sakai).

https://doi.org/10.1016/j.wnsx.2023.100199
Received 4 February 2023; Accepted 19 April 2023

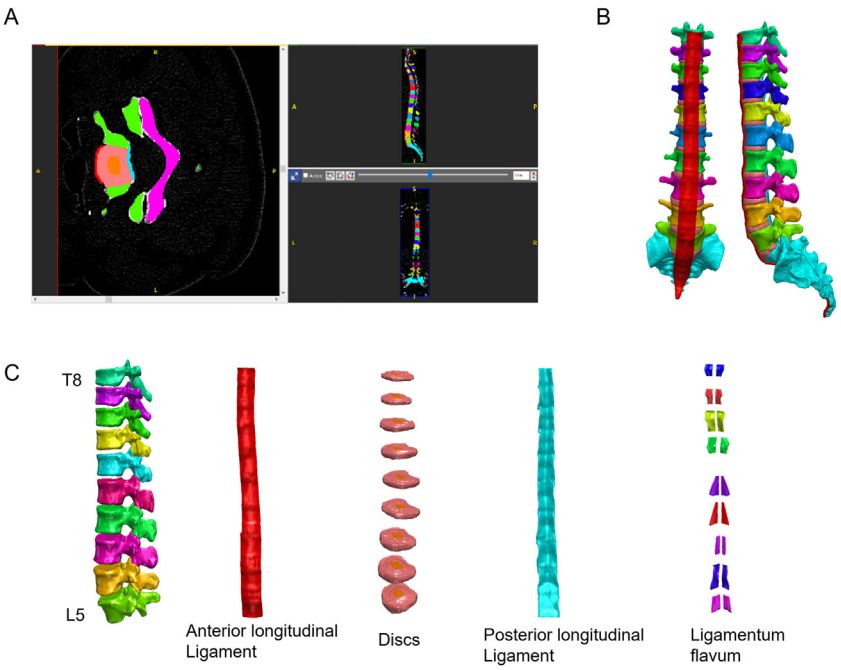

Fig. 1. (A) Each vertebral disc was mapped and (B) a spine model was created (C) from T8 to the sacrum, distinguishing each vertebral body, the anterior longitudinal ligament, intervertebral disc, the posterior longitudinal ligament, and ligamentum flavum.

Table 1
Young's modulus, Poisson ratio, and mass density.

Part	Young's modulus E [MPa]	Poisson ratio
Cortical bone (Normal)	12000	0.3
Cortical bone (Osteoorosis)	8400	0.3
Cancellous bone (Normal)	1500	0.3
Cancellous bone (Osteoorosis)	1050	0.3
Annulus fibrosus	25	0.3
Nucleus pulposus	1	0.45
Anterior longitudinal ligament	68	0.3
Posterior longitudinal ligament	96	0.3
Ligamentum flavum	28.6	0.3
Ti-6AI-4 V: rod and screw	127000	0.3

Data from Galbusera et al, Lu et al, Cowin et al, Périé et al, Ottardi et al, *and Nataranjan* et al[16–21] .

2. Methods

2.1. Patient images

Computed tomography (CT) images (slice thickness of 0.6 mm) of the spine, from the thoracic spine to the pelvis, of a 50-year-old adult woman, were obtained using the Brilliance 64 CT scanner (Philips Healthcare, Amsterdam, Netherlands). The use of these CT images was approved by the Ethics Committee at the Center for Clinical Research of the corresponding author's hospital, and written informed consent was obtained.

2.2. Model construction

Model construction was performed with FE software (simpleware ScanIP, version M-2017.06; Synopsys Inc., Mountain View, CA, USA). After the spine was extracted, vertebral bodies were mapped as cancellous and cortical bones, and interbody discs were also mapped. The cortical and cancellous bones were then separated. The computer was unable to separate the facet joints due to their small size automatically. Therefore, manual distinctions were performed while examining CT scans. A three-dimensional spine model was constructed by mapping all vertebrae and intervertebral discs from the 8th thoracic to 5th lumbar regions. Facet joint spaces were created at all levels for each vertebra to move independently. The ALL, posterior longitudinal ligament (PLL), and ligamentum flavum were added to the model (Fig. 1). In this analysis, the cranial end was T8, and the caudal side was the L5 lumbar spine. In the spine model, the total numbers of elements and nodes were 1,049,711 and 209,357, respectively.[15] In this analysis, all elements were considered to be linear elastic materials. Appropriate material properties were added to each component of the spine[16–21] (Table 1).

Thoracolumbar spine fractures are the most common fracture type of the axial skeleton, with approximately two-thirds occurring between T11 and L2[22] . In the present study, the fracture model was assumed to be at the center of T12. The wedge-shaped model was used to make a cut at T12 and ALL, assuming that the shearing force was applied to the anterior wall of the vertebral body (Fig. 2A). In the osteoporosis fracture model, we used the material properties of the cortical and cancellous bones multiplied by 0.7 (cortical bone 8400 Mpa and cancellous bone 1050 Mpa), with a bone mineral density of the Young Adult Mean of less than 70% indicating osteoporosis.[23] In the DISH fracture model, the Young's modulus of the ALL of the fracture model was changed to those of cortical bone. In the DISH-osteoporosis fracture model, the material properties of the ALL in the DISH fracture model were created by setting the data of cortical bone multiplied by 0.7. Stereolithography (STL) data on screws (ARMADA) donated by NuVasive (San Diego, USA) were used in the posterior instrumentation model. The rod connection of the screw head was removed, and a rod with a diameter of 5.5 mm was coupled to the head part (Fig. 2B). The screw diameter and length were set in the actual insertion direction by measuring the subject's vertebral body (Table 2 and Fig. 3C). Posterior fixation models were constructed for each fracture model with the following lengths: 1 vertebra above to 1 below (A1B1), two vertebrae above to 2 below (A2B2), and three vertebrae above to 3 below (A3B3). The surface of the intervertebral disc/ligament, vertebral

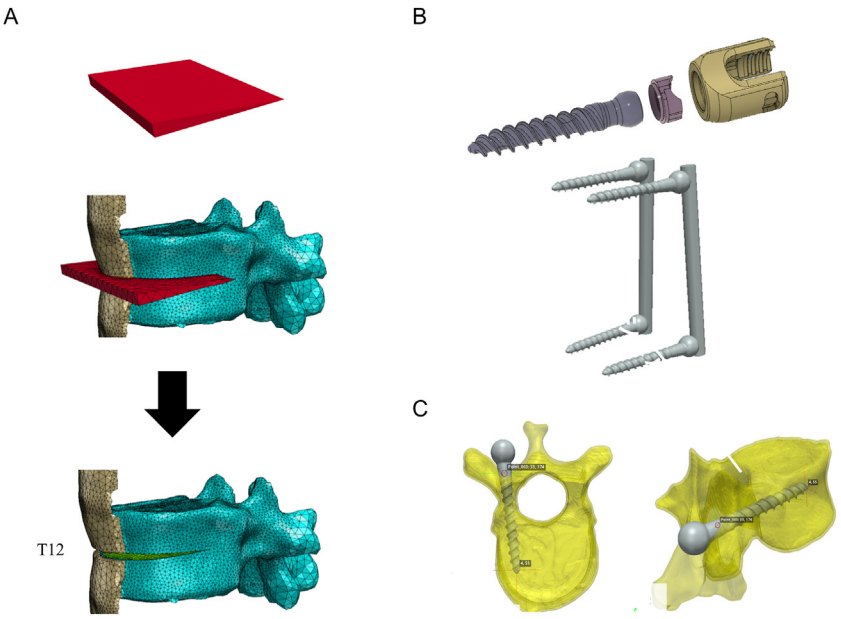

Fig. 2. (A) The fracture model was assumed to be at the center of T12, and the wedge-shaped model was used to make a cut at T12 and ALL, and (B) in the screw model, The rod connection of the screw head was removed and a rod with a diameter of 5.5 mm was coupled to the head part (C) to set the screw in each vertebra.

Table 2
Screw diameter and length of each vertebral body.

Vertebral body	Left [mm]	Right [mm]
T9	4.0 × 30	4.0 × 30
T10	4.0 × 30	4.0 × 30
T11	4.0 × 35	4.0 × 35
L1	4.0 × 35	4.0 × 35
L2	4.0 × 35	4.0 × 35
L3	5.5 × 45	5.5 × 45

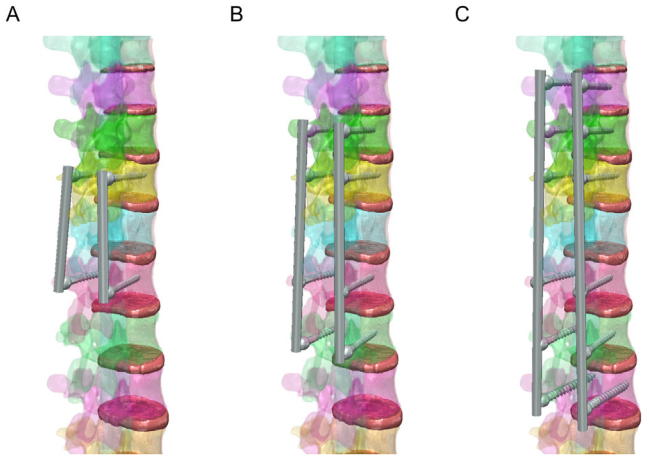

Fig. 3. Posterior fixation models were constructed for each fracture model: (A) 1 vertebrae above to 1 below (A1B1), (B) 2 vertebrae above to 2 below (A2B2), and (C) 3 vertebrae above to 3 below (A3B3).

body/intervertebral disc, screws/rods, and instrument/vertebral body were attached via the "TIE" constraint formulation in Simpleware. Moreover, all facet joints were independently constructed. And the friction of the surface was set at 0 to account for joint fluid in case of contact.

2.3. Load application

The caudal surface of L5 was constrained in the x, y, and z directions. Beam elements to two anterior points on the cranial surface of T8 and the points of both superior articular processes were made. The apex of the beam element was loaded with a moment of 1 Nm to simulate flexion and extension motions, and the entire vertebral body was loaded with 30 N as the weight loading condition (Fig. 4). Analyses were performed using Patran and MARC (MSC Software, Newport Beach, CA, USA). Thirty-two different compression combinations were evaluated, and the maximum von Mises stress values for the vertebral body, intervertebral discs, screws, and rods were recorded for each combination.

3. Results

Stress values in intervertebral discs and screws in the flexion/extension of 1A1B, 2A2B, and 3A3B fixations in the fracture model (Fig. 5), osteoporosis fracture model (Fig. 6), DISH fracture model (Fig. 7), and DISH-osteoporosis fracture model (Fig. 8) were graphically compared. Stress on fractured vertebrae (T12) increased with both flexion and extension in all fracture models. No differences were observed in stress on fractured vertebrae, other vertebrae, or intervertebral discs between the fracture and osteoporosis fracture models with a normal ALL. The fracture model and osteoporosis fracture model showed higher stress on the vertebrae and lower stress on the intervertebral disc. The DISH fracture model and DISH-osteoporosis fracture model showed lower stress on the vertebrae and higher stress on the intervertebral disc.

In all fixation models, as the screw fixation length increased, stress at the fracture level decreased. Stress on the vertebral body and intervertebral disc between the fixation lengths of the screws also decreased in all models. However, stress on the vertebral body at the cranial and caudal ends of the screws increased in all models with 1A1B, 2A2B, and 3A3B, particularly at the caudal end. Stress on the vertebrae at the caudal ends of the screws for the length of fixation was higher in the fracture model and osteoporosis fracture model than in the DISH fracture model and DISH-osteoporosis fracture model.

Stress on the screw was higher in the fracture model and osteoporosis fracture model than in the DISH fracture model and DISH-osteoporosis

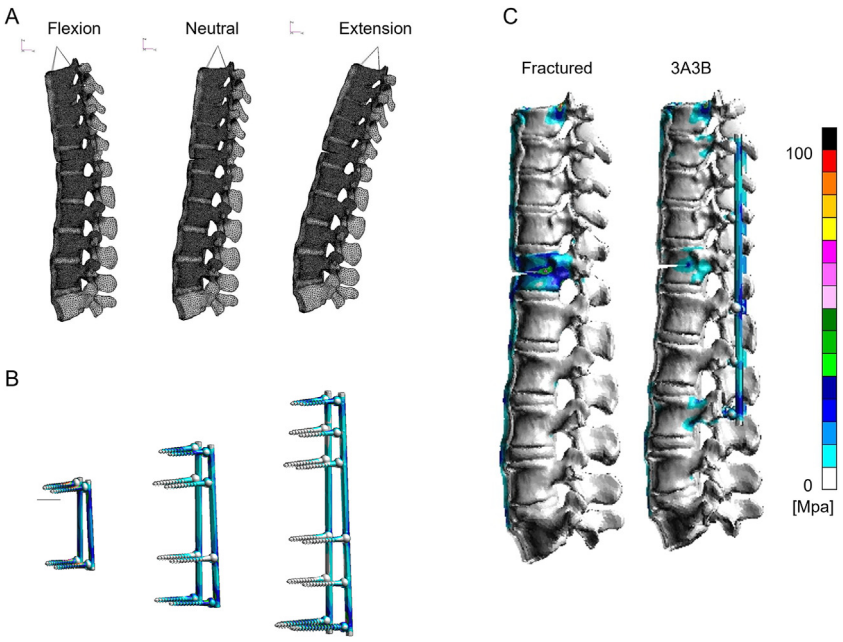

Fig. 4. The caudal surface of L5 was constrained in x, y, and z directions, and beam elements to two anterior points on the cranial surface of T8 and those of both superior articular processes were made. (A) Flexion/neutral/extension. (B) Stress diagram of a screw/rod, and (C) as an example, a stress diagram of a fractured spine and 3A3B.

fracture model. Furthermore, stress on the cranial and caudal ends of the screw increased, particularly with 1A1B, osteoporosis, and the caudal side. In the DISH fracture model and DISH-osteoporosis fracture model, although the caudal end continued to show high-stress values, stress on the screw generally decreased as the length of fixation increased, whereas that on the caudal side and at the fracture site did not markedly change between 2A2B and 3A3B. In the fracture model and osteoporosis fracture model, screw stress decreased from 1A1B to 2A2B but increased again with 3A3B. On the other hand, the stress in the rod was the lowest at 1A1B and the highest at 2A2B (Table 3).

4. Discussion

A 3D-FE spine model was created from medical images with actual screw data and stress analysis of posterior fixation was performed with the four models: vertebral fracture, osteoporosis, DISH, and DISH with osteoporosis.

Classification of thoracolumbar burst fractures was determined via the Thoracolumbar Injury Classification System (TLICS) score[24] and Thoracolumbar AO Spine Injury Score (TLAOSIS). The TLICS classification was determined by adding the scores of the three factors, including the morphology of injury, the integrity of the posterior ligamentous complex, and the neurologic status.[24] Joaquim et al reviewed that the TLICS use was safe with regards to preservation or improvement of neurologic function.[25] Santander et al reported TLAOSIS might be better for assisting surgeons in deciding on a surgical procedure on certain controversial types of fractures.[26] However, by the morphology of the fracture, posterior ligament injury, and intervertebral injury, the stresses at the fracture level would easily alter. As a result, the management of thoracolumbar burst fractures is controversial with no universally accepted treatment algorithm.[27] The primary outcomes of surgery on vertebral fractures include 1) facilitating early mobilization, which reduces the risk of complications associated with immobility and bed rest, and 2) decreasing pain medication requirements due to spinal instability.[28] Furthermore, early surgery achieves better outcomes.[29] In clinical settings, positive results of short fusion using a pedicle screw were reported for posterior fusion of vertebral fractures in the thoracolumbar transition region.[30,31] The loss of corrections of the anterior vertebral body height and implant failure in short fusion has also been demonstrated.[30] Uchida et al previously suggested that additional reinforcement with vertebroplasty for osteoporosis subjects resulted in less kyphotic loss and instrumentation failure than no vertebroplasty.[32] Ishikawa et al compared short and long posterior fixation with vertebroplasty for osteoporotic spinal collapse and found that short posterior fixation achieved good outcomes. In contrast, correction loss was less with long-segment fusion.[33] Girardo et al compared results for osteoporotic thoracolumbar vertebral fractures treated with a short or long-segment fixation. They reported positive clinical and radiological outcomes; however, long fusion achieved better kyphotic angle correction and lowered mechanical complications than short segment fusion.[34] Regarding DISH fractures, Krüger showed that a short fixation technique achieved positive outcomes in a mean postoperative follow-up of 7.9 months.[35] On the other hand, good results following the long fusion of multiple vertebrae and minimally invasive surgery were more common for kyphotic angle correction and a lower collapse rate.[36–38] The short and long fusions were discussed in terms of fixation strength and correction, with few papers describing the mechanics of pathology, length of fixation, and the effects of instrument failure. From these past studies, it is evident that vertebral fracture correction is still a controversial topic with many factors that should be considered, such as age, bone strength, fracture type, alignment, invasion, length of fixation, and whether to add a bone graft, use cross-linking devices, or hooks with open surgery.

Biomechanical analyses of thoracolumbar fractures typically involve cadaveric studies and finite element analysis. In cadaver analyses, long-segment fixation for thoracolumbar burst fractures was more stable than short-segment fixation, though it was more commonly associated with adjacent segment intervertebral damage.[39] Norton compared the outcomes of using either four pedicle screws inserted outside of the L1 fractured level or six pedicle screws, including two additional screws

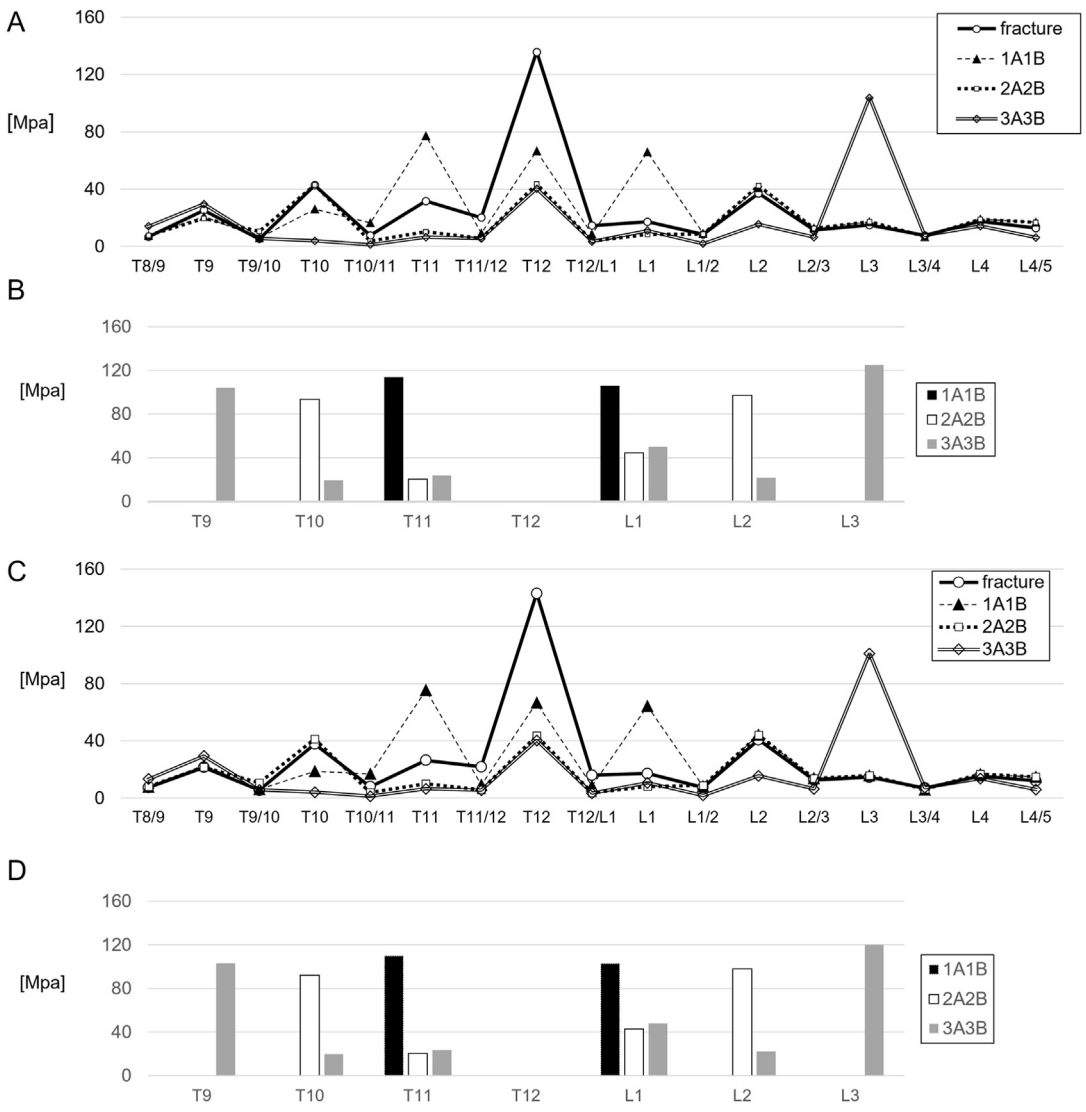

Fig. 5. The fracture model. (A) A bar chart of stress on vertebrae and intervertebral discs with flexion. (B) Stress on the respective screws with flexion of 1A1B, 2A2B, and 3A3B. (C) Bar chart of stress on vertebrae and intervertebral discs with extension. (D) Stress on respective screws with extension of 1A1B, 2A2B, and 3A3B. Vertical axis; Stress distribution (Mega Pascal; Mpa), horizontal axis; each vertebral (A, B, including each intervertebral level) level.

inserted into the broken vertebral body to improve stiffness without sacrificing the benefits of short segment fusion.[40] Liao created an FE T11-L1 spine and the posterior fusion model and reported that intervertebral mobility after fusion was higher in the osteoporotic model.[41] Two additional pedicle screws and vertebroplasty with short-segment fusion provided a stiffer construct and lower von Mises stress on the pedicle screws and rods.[42] Wang analyzed different pedicle screw models, including the cortical bone trajectory for three vertebral bodies, and detected mechanical differences in the approach used to insert screws.[43] Loenen indicated that the correction of misaligned posterior instrumentation resulted in high forces on screws and high tissue strain in adjacent and downstream spinal segments.[44] In a long fusion analysis, Joukar examined fixation for lumbosacral deficiencies.[45] In recent years, STL data created for FE analyses have been modeled using a 3D printer, and preoperative planning has been performed.[46] However, the present study is the first to use actual screw data and a long spine length to consider pathology and different fixation lengths.

In the present study, stress at the fracture level of the osteoporosis and DISH models was not much higher compared to the fractured model, though in clinical settings, bone density is decreased by osteoporosis. Since stress did not change, osteoporotic vertebral fractures may be more susceptible to collapse. On the other hand, the stress of fractured vertebrae decreased in all models after the long fixation. This may explain the better kyphosis correction and the lower collapse rate with longer fixations. Therefore, long fusion may be considered for an unstable fracture or osteoporotic bone. Stress between the vertebrae and screw was higher at the cranial/caudal end of the screw fixation length in the osteoporosis and DISH-osteoporosis models than in the fracture and DISH fracture models model, which have higher bone strength. This result is due to the screw and vertebral body being tied (the screw was sufficiently effective) in this analysis. In actual osteoporotic cases, the function of the screw is rarely sufficient. Increased stress on the screw in the present study indicates that if the load is concentrated on the instrument to assist osteoporotic fractured vertebrae, the screw is ineffective, and loosening may

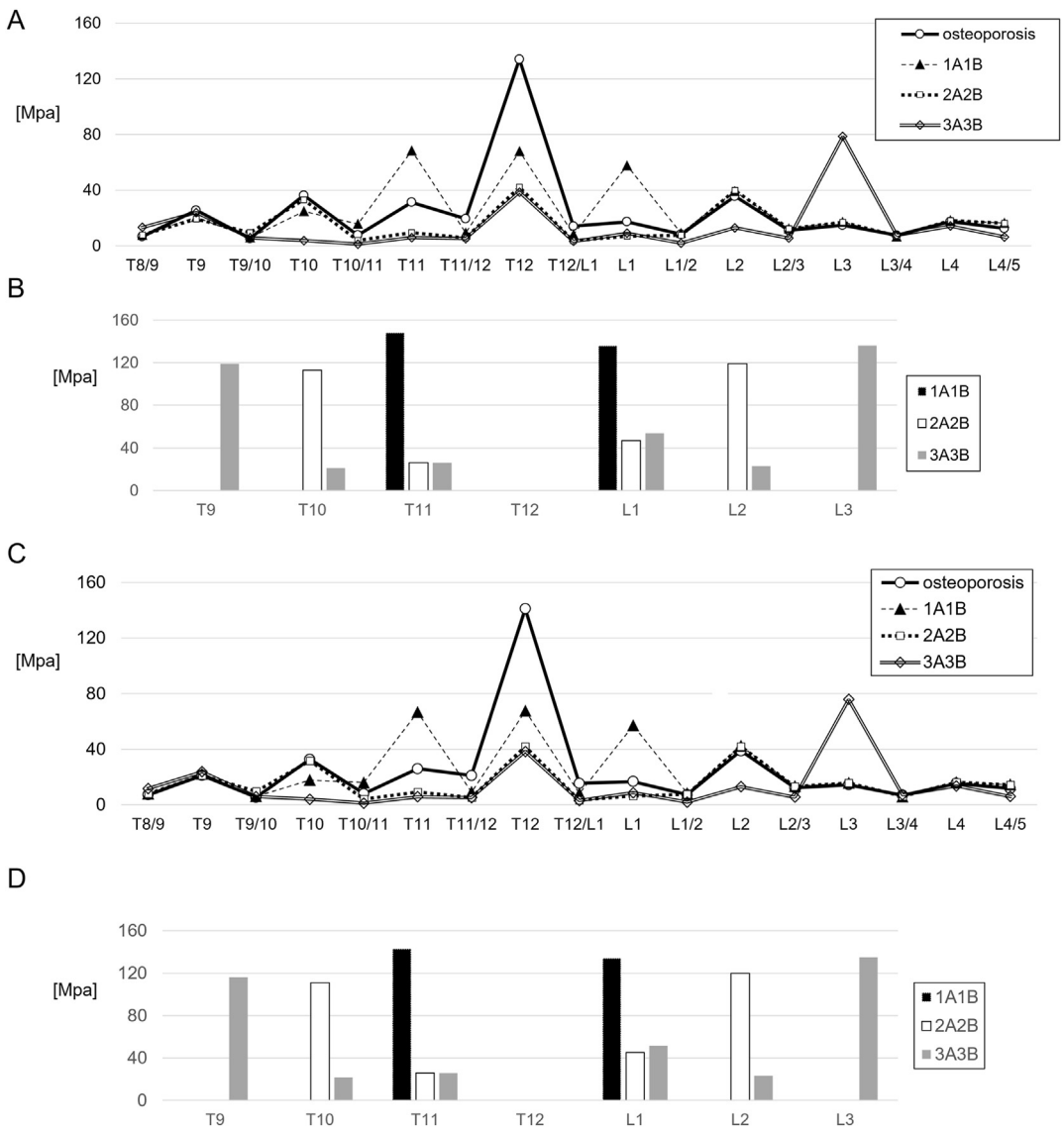

Fig. 6. The osteoporosis fracture model. (A) Bar chart of stress on vertebrae and intervertebral discs with flexion. (B) Stress on the respective screws with flexion of 1A1B, 2A2B, and 3A3B. (C) Bar chart of stress on vertebrae and intervertebral discs at extension. (D) Stress on the respective screws with extension of 1A1B, 2A2B, and 3A3B. Vertical axis; stress distribution (Mpa), horizontal axis; each vertebral (A, B, including each intervertebral level) level.

occur. In osteoporotic cases, reinforcement with tape or hooks may need to be considered, particularly at the cranial/caudal end of the screw fixation length. There is currently no information on setting the boundary condition of FE software between vertebrae and screws for osteoporosis, the torque value, or pullout strength which is a limitation that is present in the current study. The stress on fractured vertebrae of 2A2B and 3A3B fixation was lower than 1A1B and almost the same value for flexion and extension. 2A2B appeared to be superior to 3A3B with respect to stress of fractured vertebrae and screws; however, the stress on the rod was the greatest in 2A2B. The stress on the rod in 3A3B was reduced due to increased number of screws. However, the stress of screws and the caudal end vertebrae in the 3A3B fixation was high. One reason may be the close caudal end (L5) of the FE spine model. In clinical settings, it is essential to consider whether patients' load line and balance are located near the cranial/caudal side of the fixed length of long-segment fusion. Compared to the fracture and osteoporosis models with normal ALL, the DISH model showed slightly lower stress at the fracture site after fixation. Stress on the vertebrae and screws at the cranial/caudal ends of fixation was lower. This was attributed to less flexibility and mobility due to the ossification, which had a more significant effect on fractured vertebrae than on screws. On the other hand, when the material properties of the ALL had normal ligamentous properties, the stress of the screw and screw-inserted vertebrae increased. This was likely due to intervertebral mobility, which stressed the screw. In the fracture model, 1A1B effectively reduced stress at the fracture vertebrae by less than half; however, stress on the screw was high, suggesting the possibility of screw failure. In postoperative follow-ups of this type of case, careful observation for instrument failure and implant removal after bone union must be performed as early as possible. We suggest that, depending on the effectiveness of the screws, a fixation range of 1A1B for young patients with normal ALL, 2A2B with osteoporosis, and more than 2A2B with DISH may provide successful fusion. However, fixation ranges of more than 2A2B may have increased stress on the vertebrae, especially the caudal end vertebrae, and may require additional procedures such as hook and tape.

Some limitations need to be addressed. Firstly, there was only one fracture morphology as well as one type of fixation and alignment.

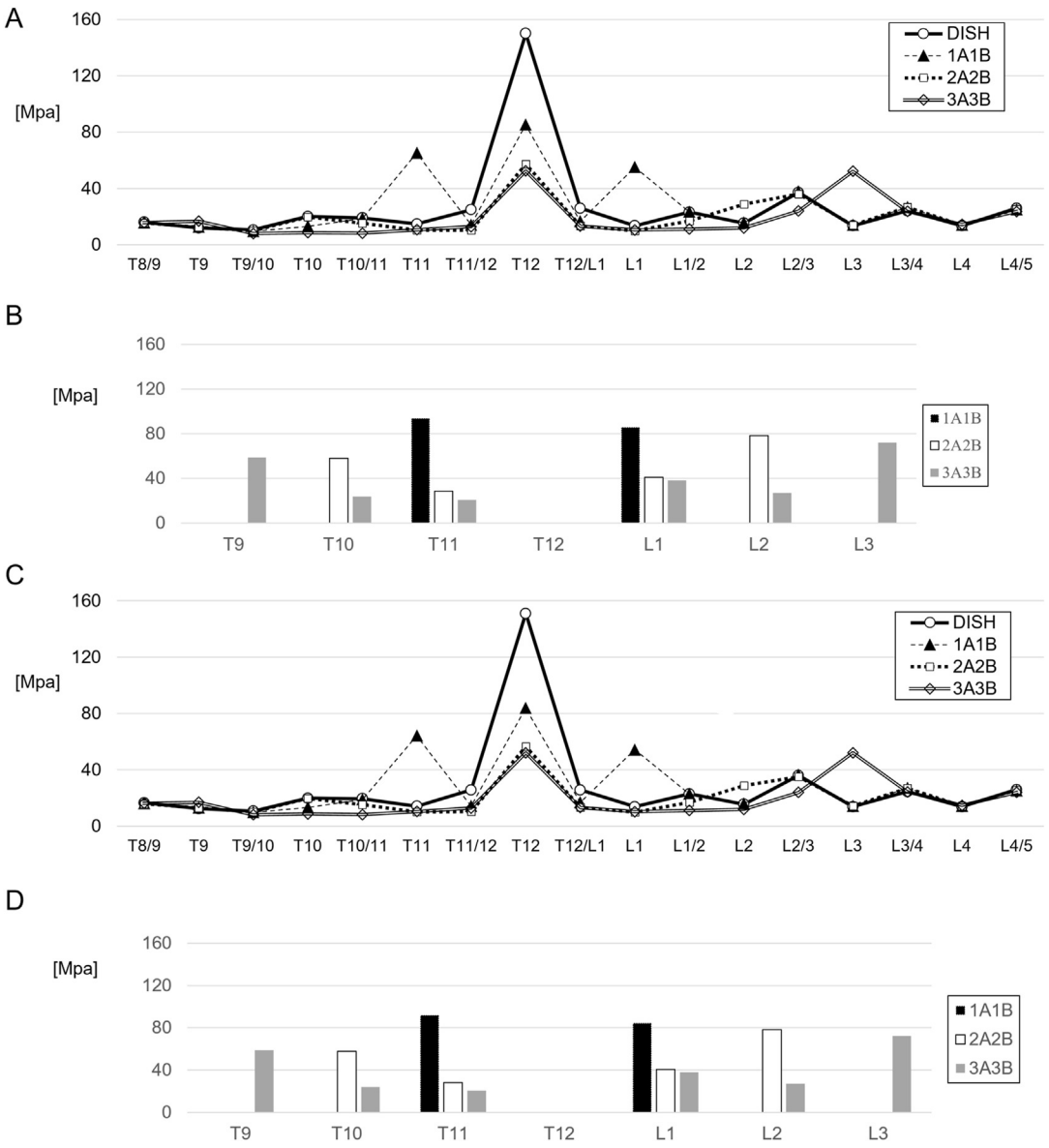

Fig. 7. The DISH fracture model. (A) Bar chart of stress on vertebrae and intervertebral discs with flexion. (B) Stress on respective screws with flexion of 1A1B, 2A2B, and 3A3B. (C) Bar chart of stress on vertebrae and intervertebral discs with extension. (D) Stress on respective screws with extension of 1A1B, 2A2B, and 3A3B. Vertical axis; Stress distribution (Mpa), horizontal axis; each vertebral (A, B, including each intervertebral level) level.

Additionally, the analysis did not consider the thoracic spine with the rib cage. The poly/fixed axial head of the pedicle screw and its interaction between the rod, screw and fixation (torque value) was not considered to save computational time. Additionally, bone strength was not considered. Muscles, facet capsules, interspinous ligament, and supraspinous ligament were also not considered. The fixation patterns (for example, three above and one below) have not yet been validated. Furthermore, screws were not inserted into fractured vertebrae. If a screw is inserted into the fractured vertebrae or a cross-link plate is used, the stress on the screw, the rod, and fractured vertebrae can change. This analysis has fewer variations in the fractured vertebral level and morphology and the number of affected vertebrae in DISH. Finally, a cadaveric biomechanical analysis has yet to be performed. However, this study is the first analysis to use actual spinal medical images and screw data to analyze different pathologies and to visualize the possible complications for multiple pathologies when varying the length of fixation. These analyses may be helpful for future research in this area.

Conclusion

The present study showed that vertebral body fracture, spinal pathology, and fixation length alter the stress on vertebrae and instrumentation, even with the same fracture morphology. Each range of fixation decreases the stress at the fractured vertebrae but affects the instrumentation and the vertebra in which the screw is inserted. The effect of fixation depends on the pathological condition, so the fixation length should be determined based on the patient's condition.

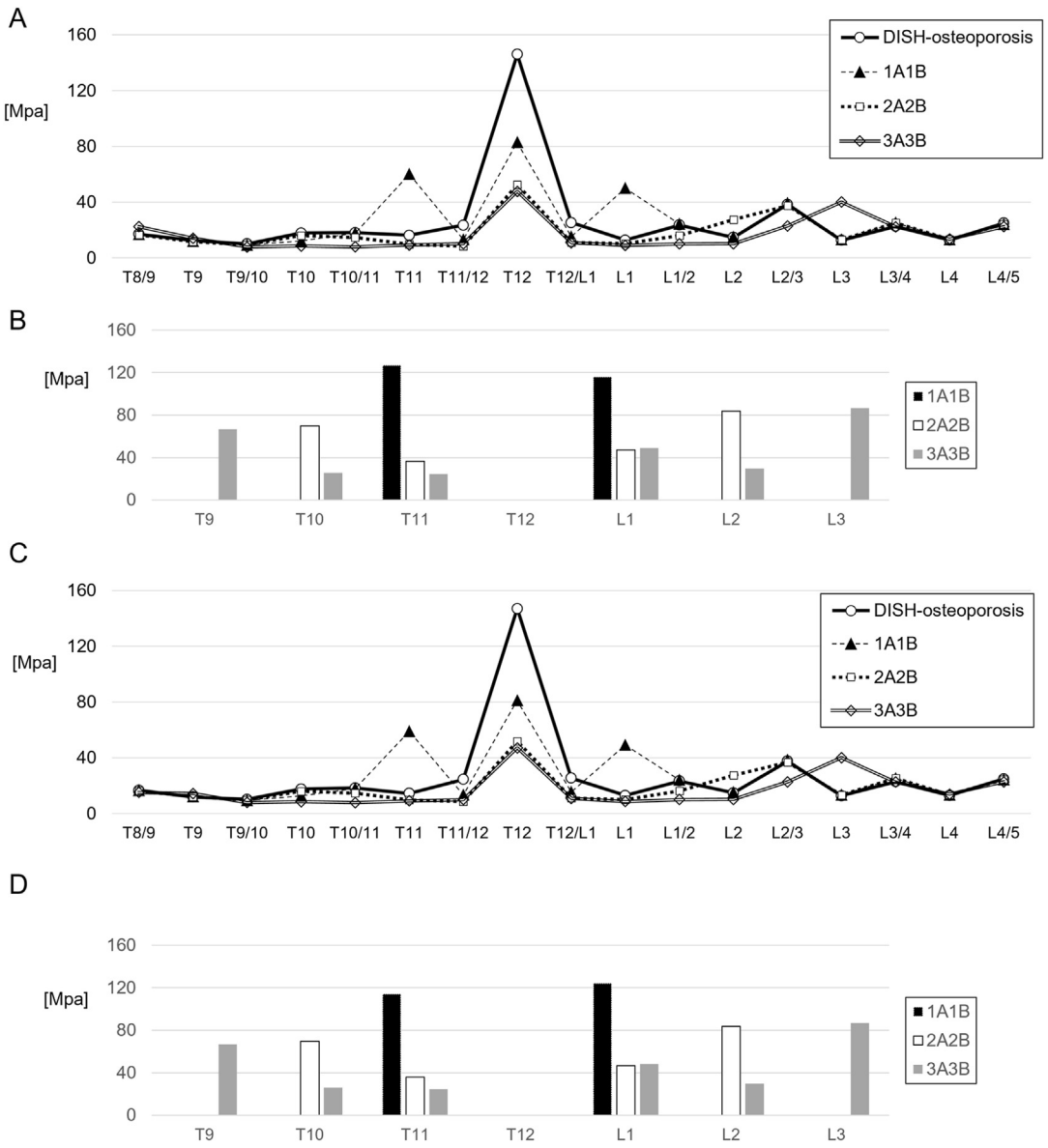

Fig. 8. The DISH-osteoporosis fracture model. (A) Bar chart of stress on vertebrae and intervertebral discs at flexion. (B) Stress of the respective screws with flexion of 1A1B, 2A2B, and 3A3B. (C) Bar chart of stress on vertebrae and intervertebral discs with extension. (D) Stress on respective screws with extension of 1A1B, 2A2B, and 3A3B. Vertical axis; Stress distribution (Mpa), horizontal axis; each vertebral (A, B, including each intervertebral level) level.

Table 3
highest rod stress distribution of rod at each model (MPa).

Flexion model	1A1B	2A2B	3A3B
the fracture model	61.6	101.0	75.9
the osteoporosis fracture model	65.6	107.0	81.2
the DISH fracture model	53.2	89.3	69.2
the DISH-osteoporosis fracture model	57.5	94.8	73.5
Extention			
model	1A1B	2A2B	3A3B
the fracture model	61.0	100.0	75.9
the osteoporosis fracture model	65.1	107.0	81.3
the DISH fracture model	53.0	89.2	69.3
the DISH-osteoporosis fracture model	57.4	94.7	73.6

Credit authorship statement

Norihiro Nishida, MD, PhD: Conceptualization, Methodology, Formal analysis, Data Curation, Writing - Original Draft, Fei Jiang, PhD: Methodology, Formal analysis, Data Curation, Rei Kitazumi, Meng: Methodology, Formal analysis, Data Curation, Yuto Yamamurara, Meng: Methodology, Formal analysis, Data Curation, Takahiro Asano, Meng: Data Curation, Rui Tome, Meng: Methodology, Formal analysis, Data Curation, Yogesh Kumaran: Writing - Review & Editing, Hidenori Suzuki, MD, PhD: Validation, Writing - Review & Editing, Masahiro Funaba, MD, PhD: Data Curation, Junji Ohgi, PhD: Methodology, Xian Chen, PhD: Supervisor, Takashi Sakai, MD, PhD: Supervisor.

Acknowledgments

Thanks to NuVasive for providing the screw STL data.

References

1. Defino HLA, Costa HRT, Nunes AA, Nogueira Barbosa M, Romero V. Open versus minimally invasive percutaneous surgery for surgical treatment of thoracolumbar spine fractures- a multicenter randomized controlled trial: study protocol. *BMC*

Muscoskel Disord. Aug 31 2019;20(1):397. https://doi.org/10.1186/s12891-019-2763-1.
2. Mallepally AR, Marathe N, Sangondimath G, Das K, Chhabra HS. Posterior stabilization without neural decompression in osteoporotic thoracolumbar fractures with dynamic cord compression causing incomplete neurological deficits. *Global Spine J.* 2020;6, 2192568220956954. https://doi.org/10.1177/2192568220956954.
3. Erichsen CJ, Heyde CE, Josten C, et al. Percutaneous versus open posterior stabilization in AOSpine type A3 thoracolumbar fractures. *BMC Musculoskelet Disord.* 2020;21(1):74. https://doi.org/10.1186/s12891-020-3099-6.
4. Liao JC, Chen WJ. Short-segment instrumentation with fractured vertebrae augmentation by screws and bone substitute for thoracolumbar unstable burst fractures. *BioMed Res Int.* 2019;2019, 4780426. https://doi.org/10.1155/2019/4780426.
5. Pellisé F, Barastegui D, Hernandez-Fernandez A, et al. Viability and long-term survival of short-segment posterior fixation in thoracolumbar burst fractures. *Spine J.* Aug 1 2015;15(8):1796–1803. https://doi.org/10.1016/j.spinee.2014.03.012.
6. Joaquim AF, Maslak JP, Patel AA. Spinal reconstruction techniques for traumatic spinal injuries: a systematic review of biomechanical studies. *Global Spine J.* 2019;9(3):338–347. https://doi.org/10.1177/2192568218767117.
7. Parker JW, Lane JR, Karaikovic EE, Gaines RW. Successful short-segment instrumentation and fusion for thoracolumbar spine fractures: a consecutive 41/2-year series. *Spine.* 2000;25(9):1157–1170. https://doi.org/10.1097/00007632-200005010-00018.
8. Lazaro BC, Deniz FE, Brasiliense LB, et al. Biomechanics of thoracic short versus long fixation after 3-column injury. *J Neurosurg Spine.* 2011;14(2):226–234. https://doi.org/10.3171/2010.10.Spine09785.
9. Agarwal N, Heary RF, Agarwal P. Adjacent-segment disease after thoracic pedicle screw fixation. *J Neurosurg Spine.* 2018;28(3):280–286. https://doi.org/10.3171/2017.6.Spine1492.
10. Granville M, Berti A, Jacobson RE. Vertebral compression fractures after lumbar instrumentation. *Cureus.* Sep 29 2017;9(9), e1729. https://doi.org/10.7759/cureus.1729.
11. Etebar S, Cahill DW. Risk factors for adjacent-segment failure following lumbar fixation with rigid instrumentation for degenerative instability. *J Neurosurg.* 1999;90(2 Suppl):163–169. https://doi.org/10.3171/spi.1999.90.2.0163.
12. Resnick D, Guerra Jr J, Robinson CA, Vint VC. Association of diffuse idiopathic skeletal hyperostosis (DISH) and calcification and ossification of the posterior longitudinal ligament. *AJR Am J Roentgenol.* 1978;131(6):1049–1053. https://doi.org/10.2214/ajr.131.6.1049.
13. Tandon V, Franke J, Kalidindi KKV. Advancements in osteoporotic spine fixation. *J Clin Orthop Trauma.* 2020;11(5):778–785. https://doi.org/10.1016/j.jcot.2020.06.028.
14. Westerveld LA, Verlaan JJ, Oner FC. Spinal fractures in patients with ankylosing spinal disorders: a systematic review of the literature on treatment, neurological status and complications. *Eur Spine J.* 2009;18(2):145–156. https://doi.org/10.1007/s00586-008-0764-0.
15. Nishida N, Jiang F, Ohgi J, et al. Biomechanical analysis of the spine in diffuse idiopathic skeletal hyperostosis: finite element analysis. *Appl Sci.* 2021;11(19):8944.
16. Galbusera F, Bellini CM, Anasetti F, Ciavarro C, Lovi A, Brayda-Bruno M. Rigid and flexible spinal stabilization devices: a biomechanical comparison. *Med Eng Phys.* 2011;33(4):490–496. https://doi.org/10.1016/j.medengphy.2010.11.018.
17. Lu YM, Hutton WC, Gharpuray VM. Can variations in intervertebral disc height affect the mechanical function of the disc? *Spine.* Oct 1 1996;21(19):2208–2216. https://doi.org/10.1097/00007632-199610010-00006. ; discussion 2217.
18. Cowin SC, Turner CH. On the relationship between the orthotropic Young's moduli and fabric. *J Biomech.* 1992;25(12):1493–1494. https://doi.org/10.1016/0021-9290(92)90062-6.
19. Périé D, Hobatho MC, Baunin C, Sales De Gauzy J. Personalised mechanical properties of scoliotic vertebrae determined in vivo using tomodensitometry. *Comput Methods Biomech Biomed Engin.* 2002;5(2):161–165. https://doi.org/10.1080/10255840290010274.
20. Ottardi C, Galbusera F, Luca A, et al. Finite element analysis of the lumbar destabilization following pedicle subtraction osteotomy. *Med Eng Phys.* 2016;38(5):506–509. https://doi.org/10.1016/j.medengphy.2016.02.002.
21. Natarajan RN, Watanabe K, Hasegawa K. Biomechanical analysis of a long-segment fusion in a lumbar spine-A finite element model study. *J Biomech Eng.* 2018;(9):140 https://doi.org/10.1115/1.4039989.
22. Magerl F, Aebi M, Gertzbein SD, Harms J, Nazarian S. A comprehensive classification of thoracic and lumbar injuries. *Eur Spine J.* 1994;3(4):184–201. https://doi.org/10.1007/bf02221591.
23. Prevention WHOSGot. *Management of O. Prevention and Management of Osteoporosis : Report of a WHO Scientific Group*. Geneva: World Health Organization; 2003.
24. Vaccaro AR, Lehman Jr RA, Hurlbert RJ, et al. A new classification of thoracolumbar injuries: the importance of injury morphology, the integrity of the posterior ligamentous complex, and neurologic status. *Spine.* 2005;30(20):2325–2333. https://doi.org/10.1097/01.brs.0000182986.43345.cb.
25. Joaquim AF, de Almeida Bastos DC, Jorge Torres HH, Patel AA. Thoracolumbar injury classification and injury severity score System: a literature review of its safety. *Global Spine J.* 2016;6(1):80–85. https://doi.org/10.1055/s-0035-1554775.
26. Santander XA, Rodríguez-Boto G. Retrospective evaluation of thoracolumbar injury classification System and thoracolumbar AO spine injury scores for the decision treatment of thoracolumbar traumatic fractures in 458 consecutive patients. *World Neurosurg.* 2021;153:e446–e453. https://doi.org/10.1016/j.wneu.2021.06.148.
27. Morrissey PB, Shafi KA, Wagner SC, et al. Surgical management of thoracolumbar burst fractures: surgical decision-making using the AOSpine thoracolumbar injury classification score and thoracolumbar injury classification and severity score. *Clin Spine Surg.* 2021;34(1):4–13. https://doi.org/10.1097/bsd.0000000000001038.
28. Kato S, Murray JC, Kwon BK, Schroeder GD, Vaccaro AR, Fehlings MG. Does surgical intervention or timing of surgery have an effect on neurological recovery in the setting of a thoracolumbar burst fracture? *J Orthop Trauma.* 2017;31(Suppl 4):S38–s43. https://doi.org/10.1097/bot.0000000000000946.
29. Ahern DP, McDonnell J, ÓD T, Butler JS. Timing of surgical fixation in traumatic spinal fractures: a systematic review. *Surgeon.* 2020;18(1):37–43. https://doi.org/10.1016/j.surge.2019.04.002.
30. Xu BS, Tang TS, Yang HL. Long-term results of thoracolumbar and lumbar burst fractures after short-segment pedicle instrumentation, with special reference to implant failure and correction loss. *Orthop Surg.* May 2009;1(2):85–93. https://doi.org/10.1111/j.1757-7861.2009.00022.x.
31. Toyone T, Ozawa T, Inada K, et al. Short-segment fixation without fusion for thoracolumbar burst fractures with neurological deficit can preserve thoracolumbar motion without resulting in post-traumatic disc degeneration: a 10-year follow-up study. *Spine (Phila Pa 1976).* 2013;38(17):1482–1490. https://doi.org/10.1097/BRS.0b013e318297bdb7.
32. Uchida K, Nakajima H, Yayama T, et al. Vertebroplasty-augmented short-segment posterior fixation of osteoporotic vertebral collapse with neurological deficit in the thoracolumbar spine: comparisons with posterior surgery without vertebroplasty and anterior surgery. *J Neurosurg Spine.* 2010;13(5):612–621. https://doi.org/10.3171/2010.5.Spine09813.
33. Ishikawa Y, Watanabe K, Katsumi K, et al. Short- versus long-segment posterior spinal fusion with vertebroplasty for osteoporotic vertebral collapse with neurological impairment in thoracolumbar spine: a multicenter study. *BMC Muscoskel Disord.* 2020;21(1):513. https://doi.org/10.1186/s12891-020-03539-0.
34. Girardo M, Massè A, Risitano S, Fusini F. Long versus short segment instrumentation in osteoporotic thoracolumbar vertebral fracture. *Asian Spine J.* 2020 https://doi.org/10.31616/asj.2020.0033.
35. Krüger A, Frink M, Oberkircher L, El-Zayat BF, Ruchholtz S, Lechler P. Percutaneous dorsal instrumentation for thoracolumbar extension-distraction fractures in patients with ankylosing spinal disorders: a case series. *Spine J.* 2014;14(12):2897–2904. https://doi.org/10.1016/j.spinee.2014.04.018.
36. Dhall SS, Wadhwa R, Wang MY, Tien-Smith A, Mummaneni PV. Traumatic thoracolumbar spinal injury: an algorithm for minimally invasive surgical management. *Neurosurg Focus.* 2014;37(1):E9. https://doi.org/10.3171/2014.5.Focus14108.
37. Okada E, Shiono Y, Nishida M, et al. Spinal fractures in diffuse idiopathic skeletal hyperostosis: advantages of percutaneous pedicle screw fixation. *J Orthop Surg.* 2019;27(2), 2309499019843407. https://doi.org/10.1177/2309499019843407.
38. Caron T, Bransford R, Nguyen Q, Agel J, Chapman J, Bellabarba C. Spine fractures in patients with ankylosing spinal disorders. *Spine (Phila Pa 1976).* 2010;35(11):E458–E464. https://doi.org/10.1097/BRS.0b013e3181cc764f.
39. McDonnell M, Shah KN, Paller DJ, et al. Biomechanical analysis of pedicle screw fixation for thoracolumbar burst fractures. *Orthopedics.* 2016;39(3):e514–e518. https://doi.org/10.3928/01477447-20160427-09.
40. Norton RP, Milne EL, Kaimrajh DN, Eismont FJ, Latta LL, Williams SK. Biomechanical analysis of four- versus six-screw constructs for short-segment pedicle screw and rod instrumentation of unstable thoracolumbar fractures. *Spine J.* 2014;14(8):1734–1739. https://doi.org/10.1016/j.spinee.2014.01.035.
41. Liao JC. Impact of osteoporosis on different type of short-segment posterior instrumentation for thoracolumbar burst fracture-A finite element analysis. *World Neurosurg.* 2020;139:e643–e651. https://doi.org/10.1016/j.wneu.2020.04.056.
42. Liao JC, Chen WP, Wang H. Treatment of thoracolumbar burst fractures by short-segment pedicle screw fixation using a combination of two additional pedicle screws and vertebroplasty at the level of the fracture: a finite element analysis. *BMC Muscoskel Disord.* 2017;18(1):262. https://doi.org/10.1186/s12891-017-1623-0.
43. Wang TN, Wu BL, Duan RM, et al. Treatment of thoracolumbar fractures through different short segment pedicle screw fixation techniques: a finite element analysis. *Orthop Surg.* 2020;12(2):601–608. https://doi.org/10.1111/os.12643.
44. Loenen ACY, Noriega DC, Ruiz Wills C, et al. Misaligned spinal rods can induce high internal forces consistent with those observed to cause screw pullout and disc degeneration. *Spine J.* 2020:30 https://doi.org/10.1016/j.spinee.2020.09.010.
45. Joukar A, Mehta J, Goel VK, Marks DS. Biomechanical analysis of the tuning fork plate versus dual pelvic screws in a sacrectomy model: a finite element study. *Global Spine J.* 2021;1, 2192568220983792. https://doi.org/10.1177/2192568220983792.
46. Wang B, Ke W, Hua W, Zeng X, Yang C. Biomechanical evaluation and the assisted 3D printed model in the patient-specific preoperative planning for thoracic spinal tuberculosis: a finite element analysis. *Front Bioeng Biotechnol.* 2020;8:807. https://doi.org/10.3389/fbioe.2020.00807.

Abbreviation list

A1B1: 1 vertebra above to 1 below
A2B2: two vertebrae above to 2 below
A3B3: three vertebrae above to 3 below
ALL: anterior longitudinal ligament
CT: Computer Tomography
DISH: diffuse idiopathic skeletal hyperostosis
FE: finite element
PLL: posterior longitudinal ligament
STL: Stereolithography